1,3-Dithiole-2-one-Fused Subphthalocyanine and Subporphyrazine: Synthesis and Properties Arising from the 1,3-Dithiole-2-one Units

Wang, Yemei
Department of Chemistry and Biochemistry, Graduate School of Engineering, Kyushu University

Uchihara, Koya
Department of Chemistry and Biochemistry, Graduate School of Engineering, Kyushu University

Mori, Shigeki
Advanced Research Support Center (ADRES), Ehime University

Furuta, Hiroyuki
Department of Chemistry and Biochemistry, Graduate School of Engineering, Kyushu University

他

出版情報：Organic Letters. 21 (9), pp.3103-3107, 2019-03-03. American Chemical Society (ACS)
バージョン：

1,3-Dithiole-2-one-fused Subphthalocyanine and Subporphyrazine: Synthesis and Properties Arising from the 1,3-Dithiole-2-one Units

Yemei Wang,[†] Koya Uchihara,[†] Shigeki Mori,[‡] Hiroyuki Furuta,*[,†,§] and Soji Shimizu*[,†,§]

[†]Department of Chemistry and Biochemistry, Graduate School of Engineering, Kyushu University, Fukuoka 819-0395, Japan

[‡]Advanced Research Support Center (ADRES), Ehime University, Matsuyama 790-8577, Japan

[§]Center for Molecular Systems (CMS), Kyushu University, Fukuoka 819-0395, Japan

Supporting Information

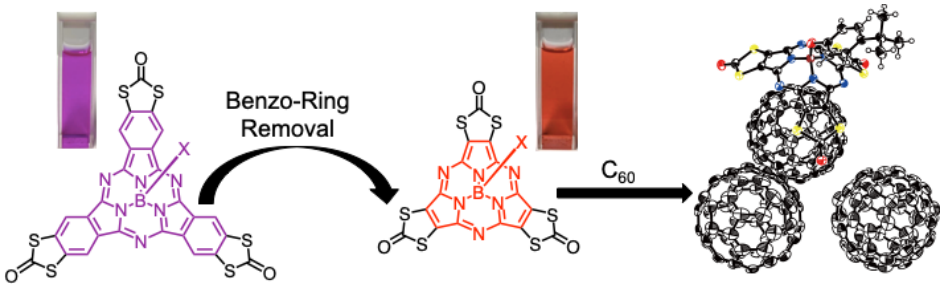

Abstract: Subphthalocyanine (SubPc) and its benzo-ring-removed analogue, subporphyrazine (SubPz), bearing 1,3-dithiole-2-one (S_2CO) groups as a new class of substituents were synthesized. In addition to the perturbed optical properties due to the presence of electron-withdrawing S_2CO units, the deep bowl-shaped structure of SubPz derivative allowed concave-convex interaction to form a unique co-crystal structure with C_{60}. Finally, using the reactivity of the peripheral S_2CO units, S_2CO-fused SubPc was successfully converted into tetrathiafulvalene (TTF)-annulated SubPc in a higher yield compared to that of the direct synthesis from a TTF-fused phthalonitrile.

Subphthalocyanine (SubPc),[1] a ring-contracted analogue of phthalocyanine comprising alternately arranged three isoindole units and imino-nitrogen bridges, has been utilized for organic electronics application due to its prominent optical and electrochemical properties arising from the 14π-electron conjugated system.[2,3] In addition, its bowl-shaped, triangular structure provides a curved π-surface for concave-convex interaction to form well-ordered multi-layers on solid surfaces and 1D columnar stackings not only in the solid state but also in solution, which are promising structural motifs for bottom-up device fabrication.[4–6] Unlike other flexible bowl-shaped molecules such as corannulene, sumanene, and so forth,[7] the stable bowl-shaped structure without inversion has found its use for molecular recognition in supramolecular chemistry[8–11] and chiroptical application in molecular chirality.[5,12,13] The three-fold molecular symmetry of SubPc can also be regarded as a useful platform for arranging functional units or expanding the conjugated systems in a C_3-symmetric manner.[14] Based on these structure-property relationships of SubPc, recently we have reported tetrathiafulvalene-annulated subphthalocyanine (TTF-SubPc), which can function as an electron donor with multi-electron redox properties arising from triply degenerate HOMO localized on the TTF units.[15] Despite its potential application in optoelectronics,[16] the yield of TTF-SubPc in our previous study was significantly low due to poor reactivity of the TTF-fused phthalonitrile precursor. During the synthesis of TTF-SubPc, we noticed that 1,3-dithiole-2-one (S_2CO)-fused phthalonitrile can serve as a precursor for the SubPc synthesis, and the resultant S_2CO-fused SubPc (S_2CO-SubPc) can further be converted into TTF-SubPc.

Herein, we developed an alternative synthesis of TTF-SubPc with an improved yield using S_2CO-SubPc. Its benzo-ring-removed congener, (S_2CO)-fused subporphyrazine (S_2CO-SubPz), was also synthesized. Besides the suitable reactivity of the S_2CO unit towards the TTF synthesis, peripheral S_2CO units provided moderate perturbation to the optical and electrochemical properties of both SubPc and SubPz. Furthermore, unique co-crystal formation of S_2CO-SubPz with C_{60} by the concave-convex interactions was revealed.

S_2CO-SubPc **2** was synthesized as an axially chloro-substituted form (**2a**) in a 14% yield from a condensation reaction of S_2CO-fused phthalonitrile **1** in the presence of BCl_3 in xylene under reflux for 5 h (Scheme 1a). Axial ligand exchange reaction of **2a** was performed in phenol at 120 °C to provide **2b**. The smaller congener of S_2CO-SubPc, S_2CO-SubPz **4**, was also synthesized from a similar reaction of S_2CO-fused maleonitrile **3** (Scheme 1b). Because **4a** could not be purified due to its low solubility, axial ligand exchange reaction was conducted by treating **4a** with phenol or 4-*tert*-butylphenol. S_2CO-SubPz was

Scheme 1. Synthesis of (a) S_2CO-SubPc **2** and (b) S_2CO-SubPz **4**

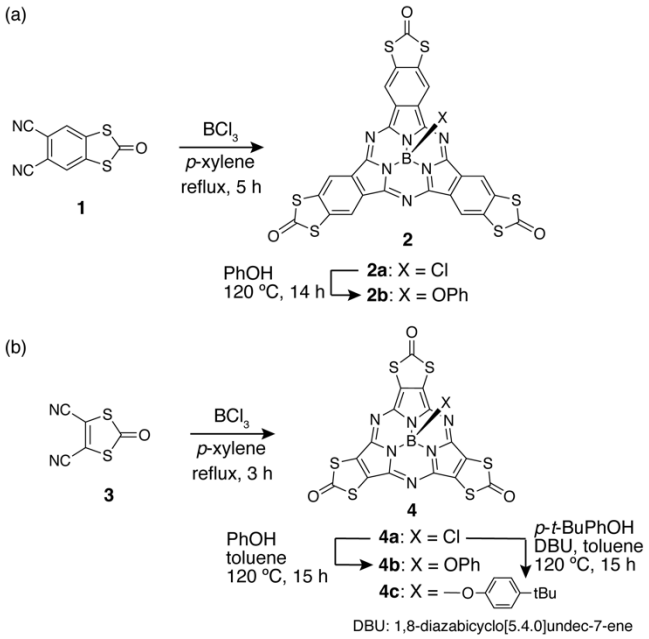

isolated as forms of **4b** and **4c** in 7.7% and 3.3% yields, respectively.

All the compounds were characterized by high resolution mass spectrometry and ^{1}H and ^{13}C NMR spectroscopies (See the Supporting Information). **2a** and **2b** both exhibited one singlet signal due to the α-benzo proton at around 9 ppm, whereas three proton signals corresponding to the phenoxy and 4-*tert*-butylphenoxy axial ligands, respectively, were observed for **2b** (6.79, 6.68, and 5.40 ppm) and S_2CO-SubPzs (**4b**: 6.85, 6.73, and 5.34 ppm; **4c**: 6.84, 5.25, and 1.13 ppm). Finally, the structures of **2a** and **4c** were unambiguously elucidated by the X-ray single crystallographic analysis (Figures 1a and 1b). Both compounds showed typical bowl-shaped geometries of SubPc and SubPz. The bowl depths estimated from the distances between the central boron and the mean-plane defined by oxygen atoms on the rim were 4.7 and 4.1 Å, respectively. The deep bowl depths and curvatures of SubPc and SubPz cores motivated us to investigate concave-convex interactions with fullerenes.[9,10,17] In the case of a combination of **4c** and C_{60}, suitable co-crystals for X-ray diffraction analysis were obtained. In the co-crystal structure, a unit cell contains one molecule of **4c**, one solvent hexane molecule, and three independent C_{60} molecules (Figure 1c). Among three C_{60} molecules, one C_{60} molecule, which exhibits concave-convex interactions with **4c**, was refined at the fixed position, whereas the others bearing side-on type π-π interactions with each other were highly disordered. In addition to the concave-convex interactions, sulfur atoms are placed in close contacts with carbon atoms of the C_{60} within the sum of van der Waals radii. This is indicative of the interaction between the electron-rich sulfur atoms and the C_{60} molecule. However, association behaviors of **2** and **4** with C_{60} in solution were not observed probably because of the electron-withdrawing nature of the S_2CO units, which decreases interaction with C_{60}. This result is in contrast to the *S*-alkyl-substituted SubPc, which is reported to form a stable complex with C_{60} in solution.[8]

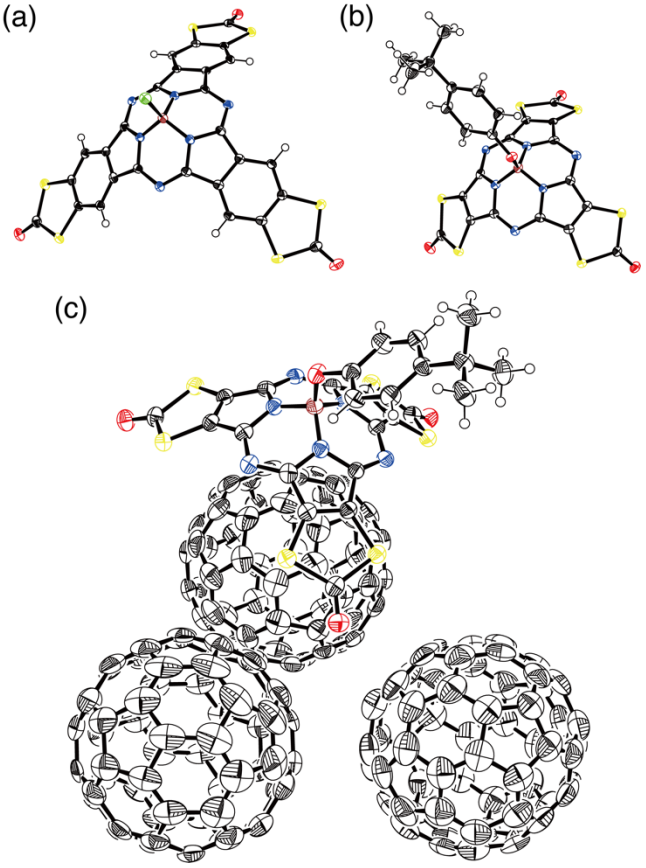

Figure 1. X-Ray single crystal structure of (a) **2a**, (b) **4c**, and (c) a co-crystal of **4c** and C_{60}. The thermal ellipsoids are scaled to the 50% probability level. In (c), a solvent hexane molecule and disordered C_{60} molecules with smaller occupancies are omitted for clarity.

Both **2** and **4** show similar UV-vis absorption spectral features to the corresponding *S*-alkyl-substituted SubPc and SubPz with moderate blue-shifts by ca. 20 nm due to the electron-withdrawing nature of the S_2CO unit (Figure 2 and Figure S13).[18,19] **2b** exhibits three characteristic absorption bands in the UV-vis region. The bands at 583 and 285 nm can be assigned as Q and Soret bands, respectively, according to the following discussion based on the magnetic circular dichroism (MCD) spectra and theoretical calculations. The broad absorption around 350 nm is typically observed for the *S*-alkyl-substituted SubPc and characterized as contribution of n-π* transition from peripheral sulfur atoms to the SubPc core.[18] The three main absorption bands of **4b** at 530, 393, and 291 nm can be similarly assigned as Q band, n-π* band, and Soret band, respectively.[19] Compared to the Q band absorption of **2b**, **4b** exhibits a blue-shift by 53 nm due to its smaller conjugated system. In contrast, the directly attached S_2CO units enhanced perturbation to the main π-conjugated system of the SubPz chromophore to intensify the n-π* transition with a red-shift by 43 nm. Unlike regular SubPz, S_2CO-fused compounds were virtually non-fluorescent due to the heavy atom effect, whereas S_2CO-SubPc **2b** exhibits intense fluorescence at 594 nm with a fluorescence quantum yield of 15% (Figure S14). Similar quenching observed for the *S*-alkyl-substituted SubPz was explained by Torres et al. in terms of the intersystem crossing from the singlet excited state to the triplet state.[20]

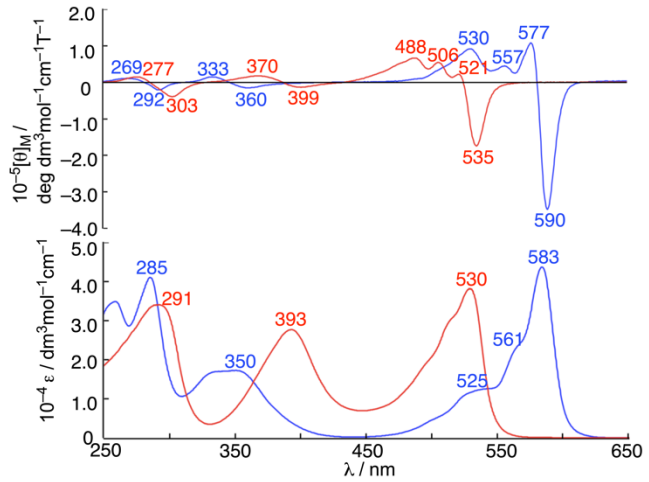

Figure 2. UV-vis absorption (bottom) and MCD (top) spectra of **2b** (blue line) and **4b** (red line) in CH_2Cl_2.

To gain the detailed insight into the electronic structures of S_2CO-compounds, MCD spectroscopy measurements and time-dependent density functional theory (TDDFT) calculations were performed. MCD spectroscopy can provide information about degeneracy of frontier orbitals based on characteristic MCD signal patterns known as a Faraday *A* term for degenerate transition and *B* terms for magnetically coupled non-degenerate transitions.[21]

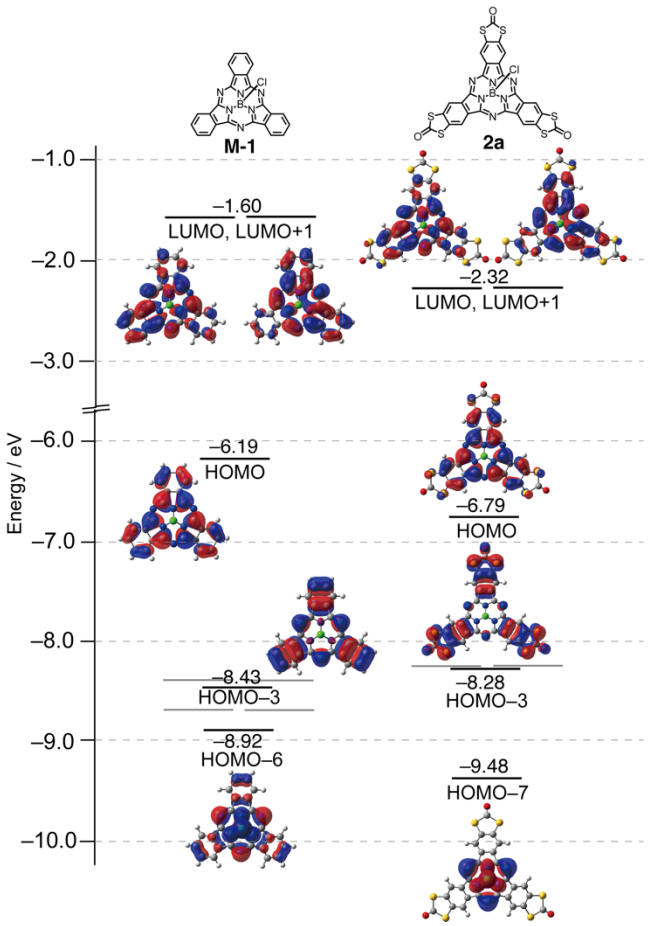

Figure 3. Partial frontier MO diagrams of **M-1** and **2a** (CAM-B3LYP/6-31G(d)).

Conventional SubPc and SubPz with three-fold molecular symmetries exhibit derivative-shaped Faraday *A* terms with an inflection point at the absorption maximum corresponding to the Soret and Q bands due to their degenerate natures. MCD sign sequences of these bands also provide information about relative magnitude differences between *Δ*HOMO and *Δ*LUMO, which refer to the energy gaps of the HOMO and the HOMO–1 (or the next HOMO of the chromophore in the case of insertion of molecular orbitals (MOs) of other origins such as metal centers and substituents) and that of the LUMO and LUMO+1, respectively. Minus-to-plus sign sequences in ascending energy are generally observed for SubPc and SubPz due to the degenerate excited state and the non-degenerate ground state (*Δ*HOMO > *Δ*LUMO).[22] The MCD spectra of both **2b** and **4b** are in good agreement with these typical MCD spectral features of symmetric SubPc and SubPz (Figure 2). The trough and peak patterns in ascending energy are observed for the Q, n-π*, and Soret bands.

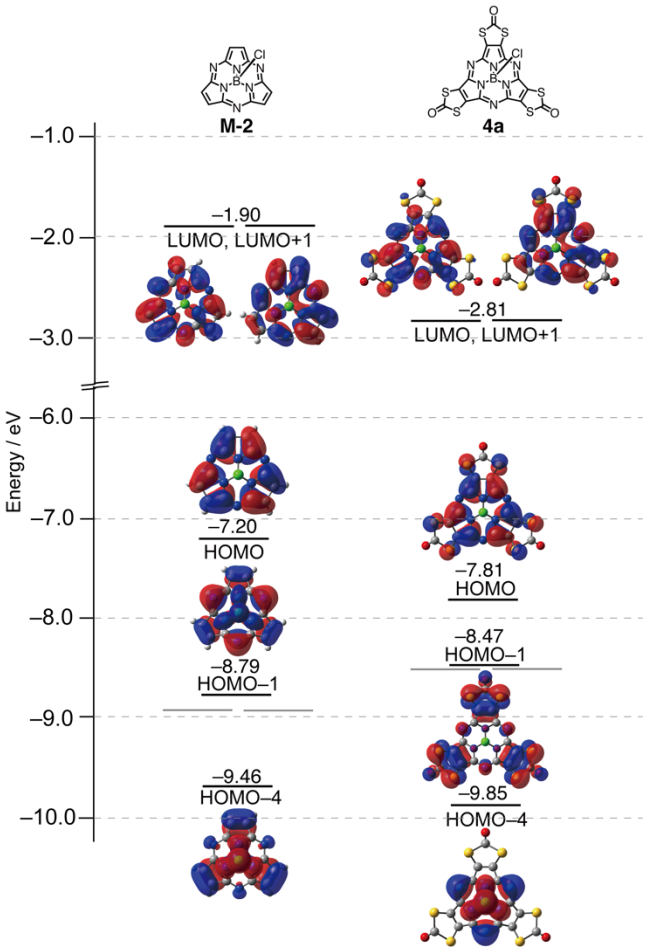

Figure 4. Partial frontier MO diagrams of **M-2** and **4a** (CAM-B3LYP/6-31G(d)).

Because of the simplicity, the axially chloro-substituted structures, **2a** and **4a**, were used as model structures for calculations. TDDFT calculations at the CAM–B3LYP/ 6-31G(d) level well reproduced the observed UV-vis absorption and MCD spectra with three major degenerate bands corresponding to the Soret, Q, and n-π* bands (Figures 3 and 4 and Tables S1–S8). n-π* transitions of **2a** and **4a** mainly consist of transitions from the HOMO–3 to the degenerate LUMO and those from HOMO–1 to the degenerate LUMO, respectively. The HOMO–7 of **2a** and

HOMO–4 of **4a** can be assigned as the next HOMO of the chromophore based on the TDDFT calculations as well as their MO distribution patterns. Compared to the MO diagrams of the corresponding non-substituted structures, **M-1** and **M-2**, the frontier MOs of **2a** and **4a** are stabilized by the electron-withdrawing S_2CO units.

The cyclic voltammogram of **2b** shows three irreversible reduction processes at –1.42 V, –1.96 V, and –2.23 V (vs. Fc^+/Fc in *o*-dichlorobenzene (*o*-DCB) containing 0.1 M tetra-*n*-butylammonium perchlorate), and one irreversible oxidation was observed at 0.74 V (Figure 5 and Figure S15). All of these oxidation and reduction potentials shift to the positive with respect to the *S*-alkyl-substituted SubPcs because of the electron-withdrawing nature of the S_2CO units.[23] In contrast, **4b** exhibits one reversible reduction followed by several reduction waves with pseudo-reversible and irreversible natures. Considering that only three reduction processes were observed for the *S*-alkyl-substituted SubPz, larger numbers of reduction processes of **4b** can be attributed to the presence of the carbonyl groups.[19a]

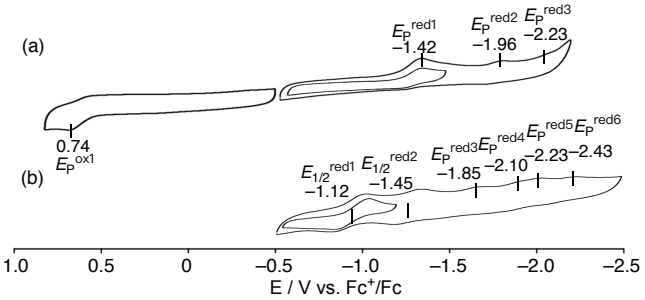

Figure 5. Cyclic voltammograms of (a) **2b** and (b) **4b** (0.5 mM) in *o*-DCB containing 0.1 M tetra-*n*-butylammonium perchlorate as a supporting electrolyte at a scan rate of 100 mV s^{-1}.

Finally, a conversion of **2a** into TTF-SubPc **6** was examined (Scheme 2). From condensation reaction of **2a** with 4,5-dithiohexyl-1,3-dithiole-2-thione in the presence of $P(OEt)_3$ in toluene under reflux, **6** was obtained in a 51% yield (Route A). The overall yield of the two-step reaction from **1** was 7%, which was improved from that of the previous synthetic route (0.7% via Route B).[15] In contrast to the successful formation of TTF-SubPc using S_2CO-SubPc, similar reactions of S_2CO-SubPzs, **4b** and **4c**, gave complicated reaction mixtures. MALDI-TOF-MS analysis revealed a larger molecular ion peak of the main product than that of the expected TTF-SubPz probably due to the side reaction, but the further structural characterization has not yet been successful.

In summary, novel S_2CO-fused SubPc and SubPz were synthesized, and their unique optical and electrochemical properties were revealed. Among these properties, multiple-electron reduction behavior of S_2CO-SubPz is of interest in view of application as an electrode-active material. Because of the deep bowl-shaped structure and the presence of sulfur atoms on the rim, S_2CO-SubPz can form a unique co-crystal structure with C_{60} molecules. Whereas the TTF forming reaction using S_2CO-SubPz and 1,3-dithiole-2-thione has not been successful due to the unexpected side reaction, which is currently under investigation, the similar reaction of S_2CO-SubPc provided the TTF-SubPc in a better yield than the previous synthetic method. This may open a wider avenue to application studies of TTF-SubPc as an electron-conducting material, which is being intensively pursued in our laboratory.

Scheme 2. Synthesis of TTF-SubPc

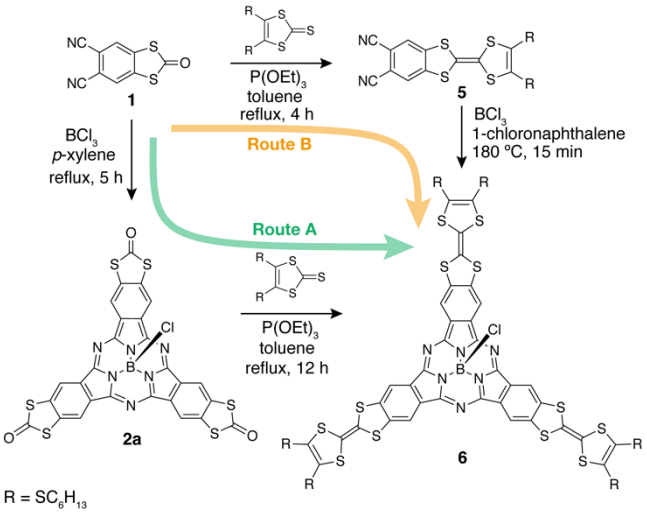

Supporting Information

The Supporting Information is available free of charge on the ACS Publications website.

Experimental procedure, ^1H and ^{13}C NMR, Crystallographic data, Cyclic voltammograms and differential pulse voltammograms, UV-vis absorption, MCD, and fluorescence spectra, and TDDFT calculation results (PDF)

AUTHOR INFORMATION

Corresponding Author

*E-mail: hfuruta@cstf.kyushu-u.ac.jp.
*E-mail: ssoji@cstf.kyushu-u.ac.jp.

ORCID

Shigeki Mori: 0000-0001-6731-2357
Hiroyuki Furuta: 0000-0002-3881-8807
Soji Shimizu: 0000-0002-2184-7468

Notes

The authors declare no competing financial interest.

ACKNOWLEDGMENT

The present work was supported by Grants-in-Aid for Young Scientists A (JSPS KAKENHI Grant Number JP26708003) and Scientific Research on Innovative Area, "π-System Figuration: Control of Electron and Structural Dynamism for Innovative Functions (No. 2601)" (JSPS KAKENHI Grant Number JP17H05160).

REFERENCES

(1) Meller, A.; Ossko, A. Phthalocyaninartige Bor-Komplexe. *Monatsh. Chem.* **1972**, *103*, 150–155.

(2) (a) Claessens, C. G.; González-Rodríguez, D.; Rodríguez-Morgade, M. S.; Medina, A.; Torres, T. Subphthalocyanines, Subporphyrazines, and Subporphyrins: Singular Nonplanar Aromatic Systems. *Chem. Rev.* **2014**, *114*, 2192–2277. (b) Claessens, C. G.; González-Rodríguez, D.; Torres, T. Subphthalocyanines: Singular Nonplanar Aromatic Compounds-Synthesis, Reactivity, and Physical Properties. *Chem. Rev.* **2002**, *102*, 835–853.

(3) (a) Morse, G. E.; Bender, T. P. Boron Subphthalocyanines as Organic Electronic Materials. *ACS Appl. Mater. Interfaces* **2012**, *4*,

5055–5068. (b) Castrucci, J. S.; Josey, D. S.; Thibau, E.; Lu, Z. H.; Bender, T. P. Boron Subphthalocyanines as Triplet Harvesting Materials within Organic Photovoltaics. *J. Phys. Chem. Lett.* **2015**, *6*, 3121–3125.

(4) Rodríguez-Morgade, M. S.; Claessens, C. G.; Medina, A.; González-Rodríguez, D.; Gutierrez-Puebla, E.; Monge, A.; Alkorta, I.; Elguero, J.; Torres, T. Synthesis, Characterization, Molecular Structure and Theoretical Studies of Axially Fluoro-Substituted Subazaporphyrins. *Chem. - Eur. J.* **2008**, *14*, 1342–1350.

(5) Guilleme, J.; Mayoral, M. J.; Calbo, J.; Aragó, J.; Viruela, P. M.; Ortí, E.; Torres, T.; González-Rodríguez, D. Non-Centrosymmetric Homochiral Supramolecular Polymers of Tetrahedral Subphthalocyanine Molecules. *Angew. Chem., Int. Ed.* **2015**, *54*, 2543–2547.

(6) Shimizu, S.; Nakano, S.; Kojima, A.; Kobayashi, N. A Core-Expanded Subphthalocyanine Analogue with a Significantly Distorted Conjugated Surface and Unprecedented Properties. *Angew. Chem., Int. Ed.* **2014**, *53*, 2408–2412.

(7) (a) Saito, M.; Shinokubo, H.; Sakurai, H. Figuration of bowl-shpaed π-conjugated molecules: properties and functions. *Mater. Chem. Front.* **2018**, *2*, 635–661. (b) Amaya, T.; Hirao, T. A Molecular Bowl Sumanene. *Chem. Commun.* **2011**, *47*, 10524–10535. (c) Wu, Y.-T.; Siegel, J. S. Aromatic Molecular-Bowl Hydrocarbons: Synthetic Derivatives, Their Structures, and Physical Properties. *Chem. Rev.* **2006**, *106*, 4843–4867.

(8) Sánchez-Molina, I.; Claessens, C. G.; Grimm, B.; Guldi, D. M.; Torres, T. Trapping Fullerenes with Jellyfish-Like Subphthalocyanines. *Chem. Sci.* **2013**, *4*, 1338–1344.

(9) (a) Nakano, S.; Kage, Y.; Furuta, H.; Kobayashi, N.; Shimizu, S. Pyrene-Bridged Boron Subphthalocyanine Dimers: Combination of Planar and Bowl-Shaped π-Conjugated Systems for Creating Uniquely Curved π-Conjugated Systems. *Chem. - Eur. J.* **2016**, *22*, 7706–7710. (b) Shimizu, S.; Nakano, S.; Hosoya, T.; Kobayashi, N. Pyrene-Fused Subphthalocyanine. *Chem. Commun.* **2011**, *47*, 316–318.

(10) (a) Sánchez-Molina, I.; Grimm, B.; Krick Calderon, R. M.; Claessens, C. G.; Guldi, D. M.; Torres, T. Self-Assembly, Host–Guest Chemistry, and Photophysical Properties of Subphthalocyanine-Based Metallosupramolecular Capsules. *J. Am. Chem. Soc.* **2013**, *135*, 10503–10511. (b) Claessens, C. G.; Torres, T. Inclusion of C_{60} Fullerene in a M_3L_2 Subphthalocyanine Cage. *Chem. Commun.* **2004**, 1298–1299. (c) Claessens, C. G.; Torres, T. Chiral Self-Discrimination in a M_3L_2 Subphthalocyanine Cage. *J. Am. Chem. Soc.* **2002**, *124*, 14522–14523.

(11) (a) González-Rodríguez, D.; Carbonell, E.; Rojas, G. d. M.; Castellanos, C. A.; Guldi, D. M.; Torres, T. Activating Multistep Charge-Transfer Processes in Fullerene−Subphthalocyanine−Ferrocene Molecular Hybrids as a Function of π−π Orbital Overlap. *J. Am. Chem. Soc.* **2010**, *132*, 16488–16500. (b) González-Rodríguez, D.; Carbonell, E.; Guldi, D. M.; Torres, T. Modulating Electronic Interactions between Closely Spaced Complementary π Surfaces with Different Outcomes: Regio- and Diastereomerically Pure Subphthalocyanine–C_{60} Tris Adducts. *Angew. Chem., Int. Ed.* **2009**, *48*, 8032–8036.

(12) Claessens, C. G.; Torres, T. Subphthalocyanine Enantiomers: First Resolution of a C_3 Aromatic Compound by HPLC. *Tetrahedron Lett.* **2000**, *41*, 6361–6365.

(13) (a) Shimizu, S.; Miura, A.; Khene, S.; Nyokong, T.; Kobayashi, N. Chiral 1,2-Subnaphthalocyanines. *J. Am. Chem. Soc.* **2011**, *133*, 17322–17328. (b) Kobayashi, N.; Nonomura, T. First Observation of the Circular Dichroism Spectra of Chiral Subphthalocyanines with C_3 symmetry. *Tetrahedron Lett.* **2002**, *43*, 4253–4255.

(14) Kamino, B. A.; Bender, T. P. Modified Boron Subphthalocyanines with Stable Electrochemistry and Tunable Bandgaps. *Dalton Trans.* **2013**, *42*, 13145–13150.

(15) Shimizu, S.; Yamazaki, Y.; Kobayashi, N. Tetrathiafulvalene-Annulated Subphthalocyanines. *Chem. - Eur. J.* **2013**, *19*, 7324–7327.

(16) Jana, A.; Ishida, M.; Park, J. S.; Bähring, S.; Jeppesen, J. O.; Sessler, J. L. Tetrathiafulvalene- (TTF-) Derived Oligopyrrolic Macrocycles. *Chem. Rev.* **2017**, *117*, 2641–2710.

(17) Konarev, D. V.; Troyanov, S. I.; Lyubovskaya, R. N. Coordination Complex of Boron Subphthalocyanine (BSubPc) with Fluorenone Pinacolate: Effective π–π Interaction of Concave BSubPc Macrocycle with Fullerene C_{60}. *CrystEngComm.* **2015**, *17*, 3923–3926.

(18) del Rey, B.; Keller, U.; Torres, T.; Rojo, G.; Agullo-Lopez, F.; Nonell, S.; Martí, C.; Brasselet, S.; Ledoux, I.; Zyss, J. Synthesis and Nonlinear Optical, Photophysical, and Electrochemical Properties of Subphthalocyanines. *J. Am. Chem. Soc.* **1998**, *120*, 12808–12817.

(19) (a) Higashino, T.; Rodríguez-Morgade, M. S.; Osuka, A.; Torres, T. Peripheral Arylation of Subporphyrazines. *Chem. - Eur. J.* **2013**, *19*, 10353–10359. (b) Rodríguez-Morgade, M. S.; Esperanza, S.; Tomas, T.; Barberá, J. Synthesis, Characterization, and Properties of Subporphyrazines: A New Class of Nonplanar, Aromatic Macrocycles with Absorption in the Green Region. *Chem. - Eur. J.* **2005**, *11*, 354–360.

(20) Rahman, G. M. A.; Lüders, D.; Rodríguez-Morgade, M. S.; Caballero, E.; Torres, T.; Guldi, D. M. Physicochemical Characterization of Subporphyrazines-Lower Subphthalocyanine Homologues. *ChemSusChem.* **2009**, *2*, 330–335.

(21) (a) Kobayashi, N.; Muranaka, A.; Mack, J. Circular Dichroism and Magnetic Circular Dichroism Spectroscopy for Organic Chemists. Royal Society of Chemistry: UK, **2012**. (b) Mack, J.; Stillman, M. J.; Kobayashi, N. Application of MCD spectroscopy to porphyrinoids. *Coord. Chem. Rev.* **2007**, *251*, 429–453.

(22) Michl, J. Magnetic Circular Dichroism of Cyclic π-Electron Systems. 1. Algebraic Solution of the Perimeter Model for the A and B terms of High-Symmetry Systems with a (4N + 2)-Electron [n]Annulene Perimeter. *J. Am. Chem. Soc.* **1978**, *100*, 6801–6811.

(23) Iglesias, R. S.; Claessens, C. G.; Torres, T.; Herranz, M. Á.; Ferro, V. R.; García de la Vega, J. M. Subphthalocyanine-Fused Dimers and Trimers: Synthetic, Electrochemical, and Theoretical Studies. *J. Org. Chem.* **2007**, *72*, 2967–2977.